


Article

Numerical Study of Mixed Convection in a Channel Filled with a Porous Medium

Filiz Ozgen ^{1,*} and Yasin Varol ² ¹ Department of Mechanical Engineering, Technology Faculty, Firat University, 23119 Elazig, Turkey² Department of Automotive Engineering, Technology Faculty, Firat University, 23119 Elazig, Turkey; yvarol@gmail.com

* Correspondence: filizozgen@gmail.com; Tel.: +90-505-478-7755

Received: 29 November 2018; Accepted: 4 January 2019; Published: 9 January 2019



Abstract: The heat transfer of mixed convection in a horizontal channel filled with a porous medium has been studied in this article, given that it plays an extensive role in various technical applications, such as flow of fluid in geothermal resources, formations in chemical industries, the storage of radioactive nuclear waste material, and cooling. Those equations written in a dimensionless form have been solved using the finite difference method for different values of the parameters. The results obtained from the study have been presented through streamlines, isotherms, and both local and average Nusselt numbers. It has been observed that parameters such as the Rayleigh and Peclet numbers have an effect on flow and temperature fields.

Keywords: Mixed heat transfer; channel; porous medium

1. Introduction

Natural or mixed convection on a heated layer in a porous medium is a frequently discussed subject. Natural convection heat transfer and fluid flow have been widely investigated in various engineering applications such as solar collectors, drying processes, fire control, geophysics, formations in chemical industries, the storage of radioactive nuclear waste, cooling, and geothermal applications. Numerous investigations on the subject moreover have a wide presence in the literature [1–7].

Cimpean and Pop [8] examined the effects of the Peclet number by studying mixed convection in a porous horizontal channel. They obtained analytical solution porous layers at low Rayleigh number conditions. Moutsoglou et al. [9] analytically studied the effects of mixed convection on a flat horizontal layer. The horizontal surface has either been down-feed heated or up-feed cooled. The developing equations were solved using the finite difference method after they have been converted into dimensionless form. Saeid and Mohamad [10] numerically studied the mixed convection within a down-feed heated horizontal channel filled with a porous medium. They had found that Rayleigh and/or the average Nusselt number had increased when the Peclet number was high. Elbasheshy [11] investigated the heat characteristics of laminar mixed convection on a horizontal flat plate inserted into a porous medium. Varol et al. [12] numerically and experimentally examined the laminar natural convection in a cavity heated from bottom due to an inclined fin. They had found that heat transfer can be controlled by attaching an inclined fin onto a wall. Kumari and Nath [13] studied the effects of radiation on the mixed convection on a horizontal surface in a porous medium, whereby it was assumed that the wall temperature had varied with the distance measured from the edge of the layer. The developing parabolic differential equations were numerically solved using the finite difference method. It was pointed out that heat transfer is strongly influenced by the number of radioactive flow, the temperature change of the wall, the non-dimensional Darcy parameter, and the free flow rate. Pop et al. [14] theoretically studied mixed convection in a narrow vertical pipe filled with a porous

medium. Their numerical results had revealed that the analytical and asymptotic solutions were in very good accord. Guerroudj and Kahalerras [15] numerically studied laminar mixed convection in a two-dimensional parallel straight channel filled with porous blocks of varying shapes, and presented the parameters affecting that heat transfer through graphs. Khanafer and Chamkha [16] studied mixed convection in a horizontal circuit that produces porous heat, whereupon the external cylinder was cooled, whilst the internal cylinder was heated. What had resulted was the formation of forced convection due to the cool external cylinder at a fixed angle speed. The obtained results had shown that the Richardson number had had an effect upon such flows in the circuit. Similar studies have also been produced and published by Muthuraj and Srinivas [17], Kumari [18], Nosonov and Sherement [19], Saeid and Pop [20] and Saeid [21].

In this study, mixed convection heat transfer was studied in a channel filled with a porous medium. Streamlines, isotherms, local and mean Nusselt numbers will be presented in the following sections of the paper for different Rayleigh numbers, the Peclet number, and the location of the heat source. Unlike the literature, the heat transfer in the channel was studied by heating 1/3 of the bottom of the channel, as well as by sliding to the up-stream and down-stream equally. The channel's length has been chosen to meet these requirements, which is about 10 times greater than the channel's height. The equations used for the analysis of both the flow and the heat transfer along the channel were numerically solved via the finite difference method.

2. Mathematical Model

In this study, mixed convection heat transfer has been studied in a channel filled with a porous medium. The related geometry, boundary conditions, and coordinates are shown in Figure 1. This figure shows the coordinates and boundary conditions. The length of the bottom wall was L , and the height of the cavity was $H = L/10$. The rest of the bottom surface is adiabatic, while one third of the bottom of the channel was heated at a constant temperature. The top wall was kept at a constant cold temperature.

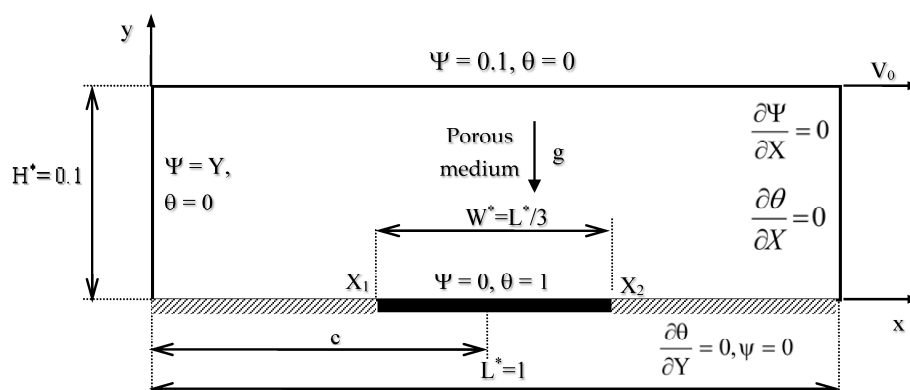


Figure 1. Schematic configuration with coordinates and boundary conditions.

The continuity, momentum, and energy equations that have become dimensionless must be solved simultaneously in order to solve problem of fluid motion and heat transfer in enclosed volumes. One can see that these are nonlinear partial differential equations, and that is impossible to solve them analytically. In order to solve obtained algebraic equations, the *Successive Under Relaxation* (SUR) method of the iterative methods had been used. Given that the convergence criterion, 10^{-5} had been selected for all of the dependent variables, the value of 0.1 is taken for under-relaxation parameter for all parameters. A 301×31 equal pitched grid distribution has been used in the x and y directions.

The dimensional governing equations for continuity, momentum and energy can be written as follow:

$$\frac{\partial u}{\partial x} + \frac{\partial v}{\partial y} = 0 \quad (1)$$

$$\frac{\partial u}{\partial x} - \frac{\partial v}{\partial y} = -\frac{g\beta K}{\gamma} \frac{\partial T}{\partial x} \quad (2)$$

$$u \frac{\partial T}{\partial x} + v \frac{\partial T}{\partial y} = \alpha \left(\frac{\partial^2 T}{\partial x^2} + \frac{\partial^2 T}{\partial y^2} \right) \quad (3)$$

In order to write Equations (1)–(3) in dimensionless form, the following dimensionless statements have been used;

$$X = \frac{x}{L}, Y = \frac{y}{L}, U = \frac{u}{V_0} = \frac{\partial \Psi}{\partial Y}, V = \frac{v}{V_0} = -\frac{\partial \Psi}{\partial X} \quad (4)$$

$$\theta = \frac{T-T_c}{T_h-T_c}, \quad \frac{g\beta K(T_h-T_c)L}{\gamma \alpha}, Pe = \frac{\gamma_0 L}{\alpha}$$

which thus lead to the following dimensionless form of the governing equations used for the model;

$$\frac{\partial^2 \Psi}{\partial Y^2} + \frac{\partial^2 \Psi}{\partial X^2} = -\frac{Ra}{Pe} \frac{\partial \theta}{\partial X} \quad (5)$$

$$Pe \left[\frac{\partial \Psi}{\partial Y} \frac{\partial \theta}{\partial X} - \frac{\partial \Psi}{\partial X} \frac{\partial \theta}{\partial Y} \right] = \frac{\partial^2 \theta}{\partial X^2} + \frac{\partial^2 \theta}{\partial Y^2} \quad (6)$$

The finite difference method had been used for the solution to these equations. In the study, we can apply the boundary conditions for the solid wall and fluid interface as follows:

$$(X, 1) = 0.1, \theta(X, 1) = 0 \quad (7)$$

$$\Psi(0, Y) = Y, \theta(0, Y) = 0 \quad (8)$$

$$\frac{\partial \Psi(L, Y)}{\partial X} = 0, \frac{\partial \theta(L, Y)}{\partial X} = 0 \quad (9)$$

Along the part where there is a heat source;

$$0 \leq X \leq X_1, \frac{\partial \theta(X, 0)}{\partial Y} = 0, \Psi(X, 0) = 0 \quad (10)$$

$$X_2 \leq X \leq L, \frac{\partial \theta(X, 0)}{\partial Y} = 0, \Psi(X, 0) = 0 \quad (11)$$

$$X_1 \leq X \leq X_2, (X, 0) = 1, \Psi(X, 0) = 0 \quad (12)$$

The local and average Nu numbers can be given as follows:

$$Nu_x = \left(-\frac{\partial \theta}{\partial Y} \right)_{Y=0} \quad (13)$$

$$Nu = \int_0^L Nu_x dx$$

Calculations have been carried out for various Peclet and Rayleigh numbers. The influence of the Peclet and Rayleigh numbers on the temperature distribution in the rigid substance has been previously pointed out. When making the necessary observations, the heat source had slid equally to both the up-stream and down-stream in a 1/3 ratio. For different Peclet and Rayleigh numbers, the flow and temperature profiles have been given in the case that the heat source is close to the down-stream, at the center, and close to the up-stream.

The results obtained from the flow program and from the literature for the validity of the numerical solution are displayed in Table 1. In the table, the values of Nusselt number, in comparison to the literature, are consistent with the values of 1, 5, and 10 for Peclet numbers and 100 for Rayleigh number. The minimum difference between the results by Saeid and Pop [20] and the present results is 3%. The results have been found to be in accordance with the values in the literature, and can thus be used for further calculations.

Table 1. The comparison of average Nu number for $Ra = 100$ [3].

Pe	1	5	10
Saeid and Mohamad [10]	5.7	5.8	5.85
Saeid and Pop [20]	4.1	4.5	5.8
Present Study	4.23	4.27	4.8

3. Results and Discussion

Mixed convection heat transfer has been numerically studied in a channel filled with a porous medium, and whose thickness of the upper and bottom walls are negligible. The results obtained from the study are given in terms of streamlines, isotherms, and local and average Nusselt numbers. The calculations have been carried out for different Rayleigh and Peclet numbers. The Rayleigh and Peclet numbers have been found to be effective parameters on flow and heat transfer.

In Figure 2, the heat source close to the down-stream, the streamline (above), and the isotherms (below) that emerge in the enclosed volume at different values of the Rayleigh number for $Pe = 0.5$ are seen. In Figure 2a, for $Ra = 100$, there are several centers of rotation seen at the top of the heater. Because the Rayleigh number is low, the temperature curves are distributed properly. Flow field is symmetric and single cell is formed in the heat source. Right cells rotate in clockwise direction with $\Psi_{\min} = -3.26$. In other words, there is a weak clockwise circulation due to domination of conduction. The other small cell sits at the left of the heat source with $\Psi_{\max} = 3.56$.

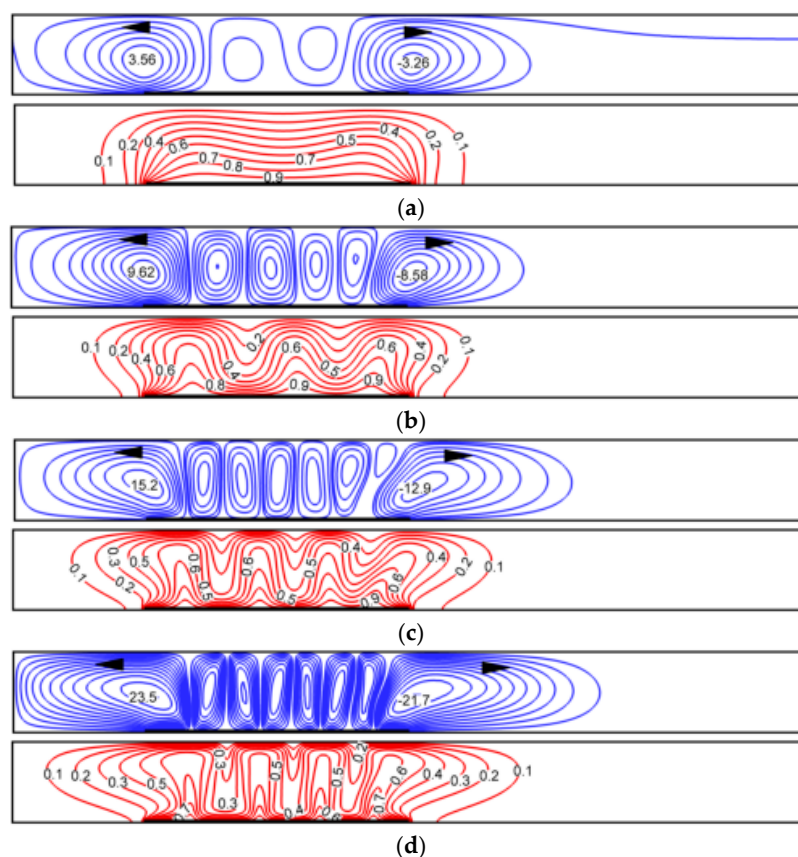


Figure 2. Streamlines (above) and isotherms (below) profiles for different Ra numbers and $Pe = 0.5$, ($c = 0.33$), (a) $Ra = 100$, (b) $Ra = 250$, (c) $Ra = 500$, (d) $Ra = 1000$.

In Figure 2b, $Ra = 250$ increases the number of rotation centers, thus causing the temperature curves to fluctuate. The values of $\Psi_{\min} = -8.58$ and $\Psi_{\max} = 9.62$. With the increase of the Rayleigh number in Figure 2c, the heated fluid on the lower surface diffuses into the closed volume, and hence

penetrates further. As is seen from the relevant temperature curves, the heat transfer through the transmission is reduced, while the heat transfer through the convection starts to dominate. This situation is more apparent in Figure 2d. The increase in the Rayleigh number intensifies the flow, increases the center of rotation within the volume, and causes the temperature curves to further penetrate the edges of the surface. For higher Rayleigh numbers, Figure 2c,d, the convection is vigorous with $\Psi_{\min} = -12.9$, $\Psi_{\max} = 15.2$ and $\Psi_{\min} = -21.7$, $\Psi_{\max} = 23.5$, respectively. However, the absolute values of minimum and maximum flow values increase.

In Figure 3, the flow-temperature profiles have been given depending on the varying Rayleigh numbers for $Pe = 1$ in the case that the heat source is close to the down-stream. For small values of Peclet number ($=0.5$), an oscillation in the temperature and flow fields is observed for a short time, after which a steady-state is reached as shown in Figure 2. For $Pe = 1$, an oscillation in the temperature and flow fields is observed, and in this value of the Peclet number there will be no steady-state flow but periodic convection state, as shown in Figure 3. As is shown in Figure 2, the flow is concentrated around the heat source, whereby numerous centers of rotation have formed for all of the Rayleigh numbers; in addition, the minimum and maximum flow function values are also given. Two or more centers of rotation have been acquired among all of the Rayleigh numbers. Some of the cells formed on the heaters rotate clockwise, whereas others rotate counterclockwise. The values of stream function are close to each other as $\Psi_{\min} = -1.56$, $\Psi_{\min} = -4.73$, $\Psi_{\min} = -7.08$ and $\Psi_{\min} = -10.4$, on the Figure 3a,d. As shown from the figure, values of $\Psi_{\max} = 1.85$, $\Psi_{\max} = 5.07$, $\Psi_{\max} = 8.07$ and $\Psi_{\max} = 12.1$. Since conductive heat transfer is effective, as is observed in the isotherms, it appears that there is no extreme change in the lower Rayleigh numbers and, moreover, there are isotherms distributing in fungi-shaped on the horizontal heater of the high Rayleigh numbers.

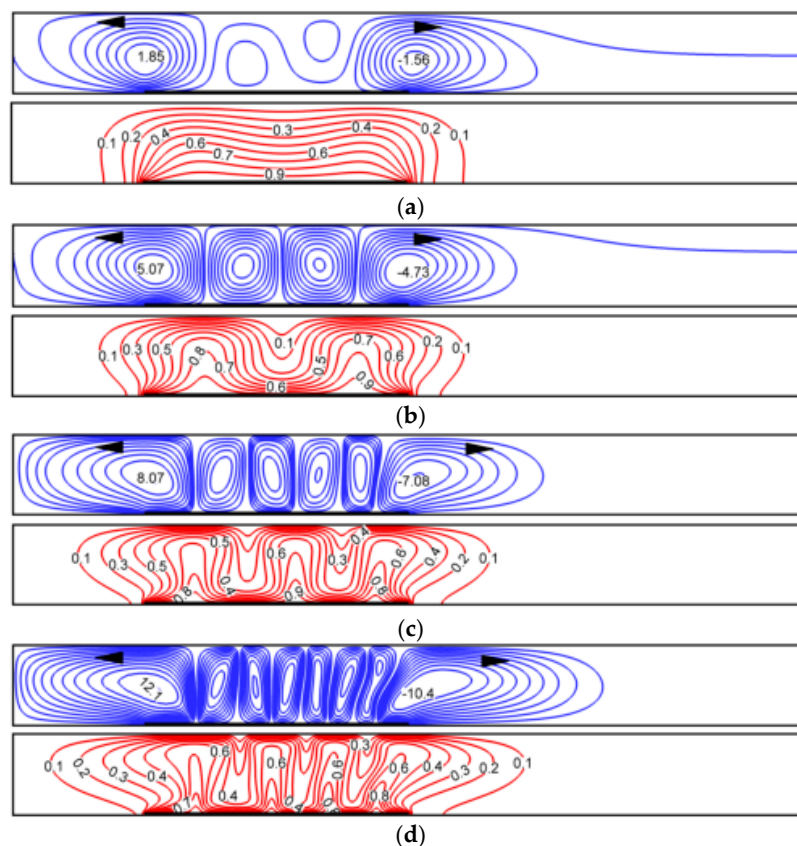


Figure 3. Streamlines (above) and isotherms (below) profiles for different Ra numbers and $Pe = 1$, ($c = 0.33$), (a) $Ra = 100$, (b) $Ra = 250$, (c) $Ra = 500$, (d) $Ra = 1000$.

In Figures 4 and 5, the flow-temperature profiles are shown depending upon the different numbers of Peclet and Rayleigh numbers in the cases where the heat source is close to the up-stream. Similar to the other positions of the heat source, the flow is concentrated around the heat source, and numerous centers of rotation have formed for all Rayleigh numbers; the minimum and maximum flow function values are also given. It can be seen from Figure 4 that $\Psi_{\max} = 3.5$, $\Psi_{\min} = -3.2$ (Figure 4a), $\Psi_{\max} = 9.6$, $\Psi_{\min} = -8.5$ (Figure 4b), $\Psi_{\max} = 15.2$, $\Psi_{\min} = -12.9$ (Figure 4c), $\Psi_{\max} = 23.5$, $\Psi_{\min} = -21.3$ (Figure 4d). Depending on the increase in the Rayleigh number, a temperature distribution in the form of a flame, especially on the heater, is acquired. In cases where the Rayleigh number is low, the fungi-shaped temperature distribution also appears to be present. The flame-shaped temperature refers to a higher convection heat transfer.

It can be seen from this Figure 5 that $\Psi_{\max} = 1.84$ when $Ra = 100$ (Figure 5a) and it increases to $\Psi_{\max} = 5.07$ when Rayleigh is increased to 250 (Figure 5b). Increasing the Rayleigh number from 500 to 1000 leads to further increase in Ψ_{\max} from 8.06 to 12.1 in Figure 5. The values of stream function are found as: $\Psi_{\min} = -1.54$, $\Psi_{\min} = -4.72$, $\Psi_{\min} = -7.04$ and $\Psi_{\min} = -10.1$, and shown in Figure 5a,d.

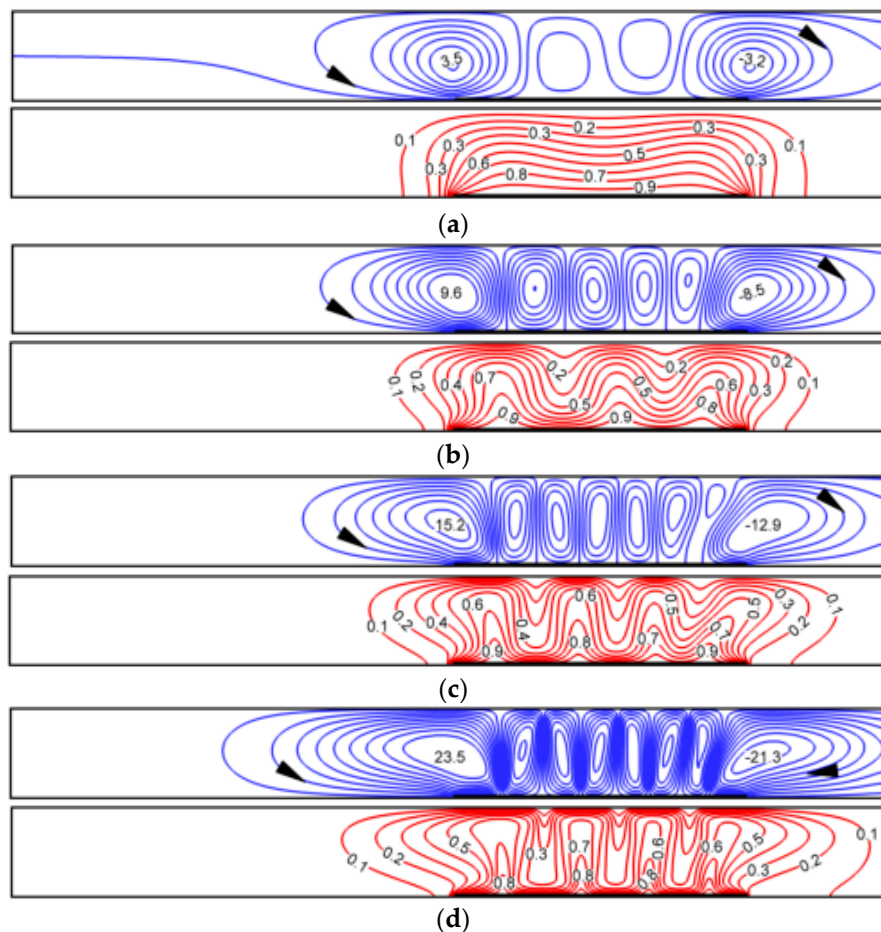


Figure 4. Streamlines (above) and isotherms (below) profiles for different Ra numbers and $Pe = 0.5$, ($c = 0.66$), (a) $Ra = 100$, (b) $Ra = 250$, (c) $Ra = 500$, (d) $Ra = 1000$.

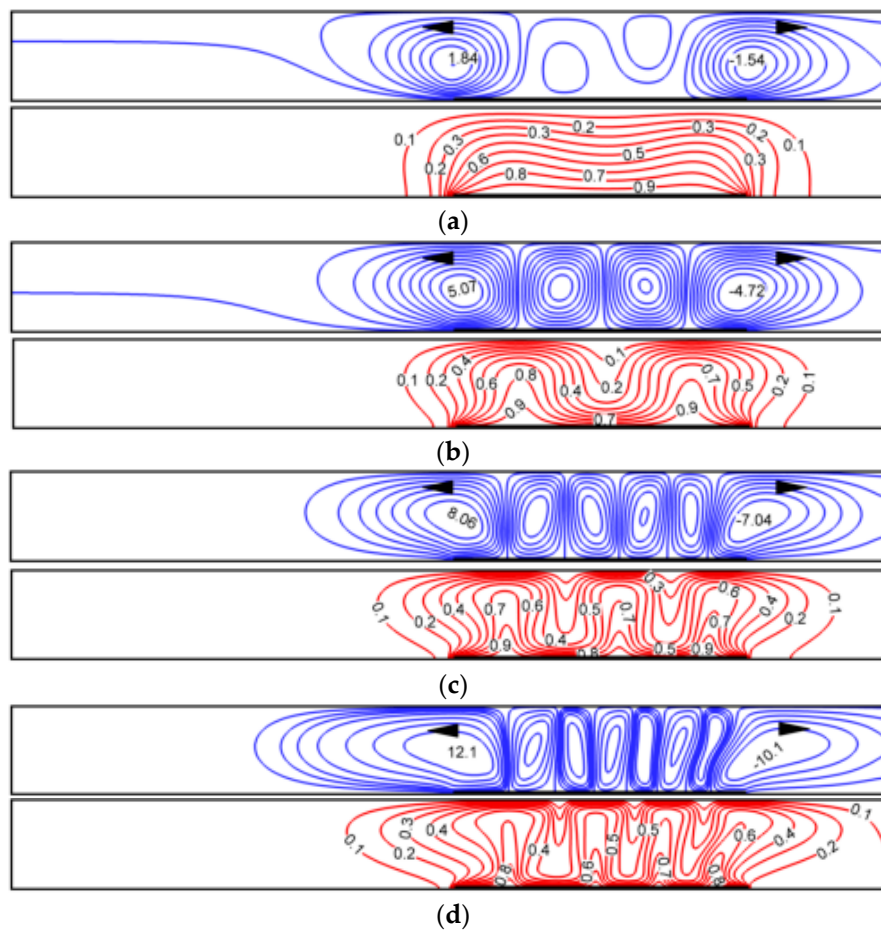


Figure 5. Streamlines (above) and isotherms (below) profiles for different Ra numbers and $Pe = 1$, ($c = 0.66$), (a) $Ra = 100$, (b) $Ra = 250$, (c) $Ra = 500$, (d) $Ra = 1000$.

In Figure 6, it can be seen that the change of the local Nusselt number is close to the down-stream, depending on the different Peclet and Rayleigh numbers. The local Nusselt numbers for all parameters represent a sinusoidal distribution. The location of the points at the highest value in the sinusoidal change can be explained by correlating it in relation to the change of flow lines in the flow and temperature profiles. The points which represent the center of rotation is influenced by the flow. Similarly the highest value of local Nusselt number is obtained at the point which is the center of rotation. The symmetrical behavior within the closed volume is disrupted as the Rayleigh number increases. In this case, the flow penetrates more into the closed volume, and the flow thus becomes activated. The increase in the Rayleigh number lets the local Nusselt number increase as well.

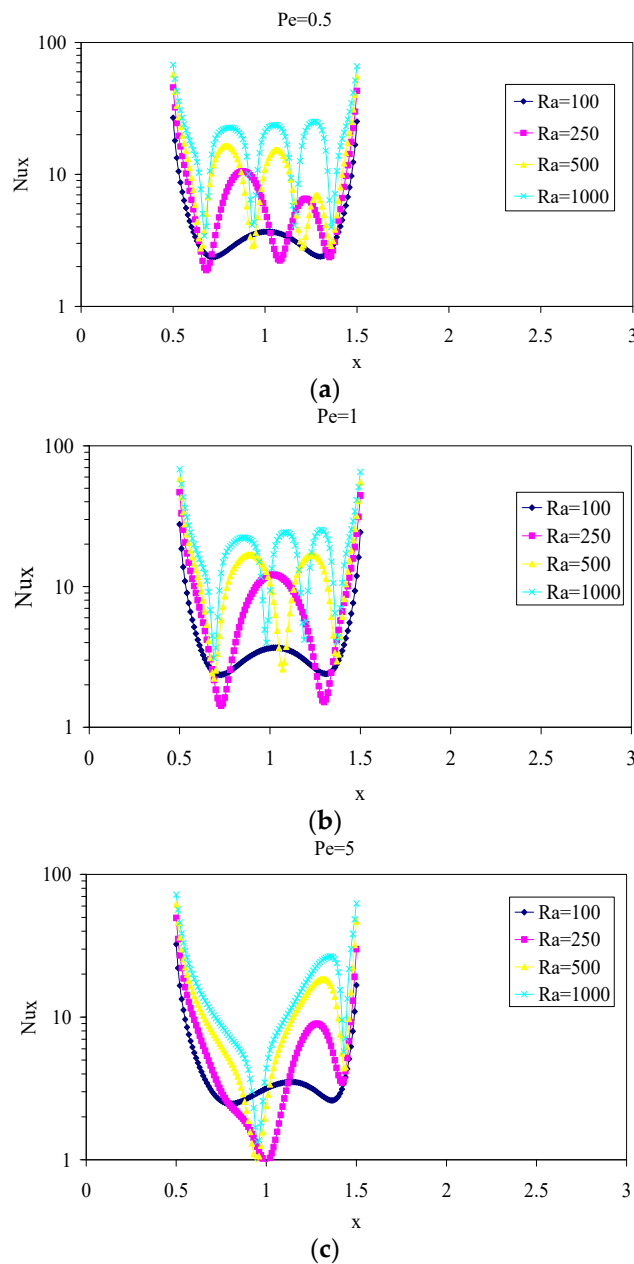


Figure 6. Variation of local Nusselt number along the channel ($c = 0.33$), (a) $Pe = 0.5$, (b) $Pe = 1$, (c) $Pe = 5$.

Figure 7 shows the change of the local Nusselt number depending on the different numbers of Peclet and Rayleigh, in the case that the heat source is close to the up-stream. The local Nusselt numbers for all of the parameters represent a sinusoidal distribution parallel to the figures given above. What is more, the location of the points at the highest value in the sinusoidal change can be explained by correlating a relation with the change of streamlines in the flow and temperature profiles. Those points with a center of rotation are influenced by the flow; and therefore the highest value in the local Nusselt number is also obtained where the center of rotation is found.

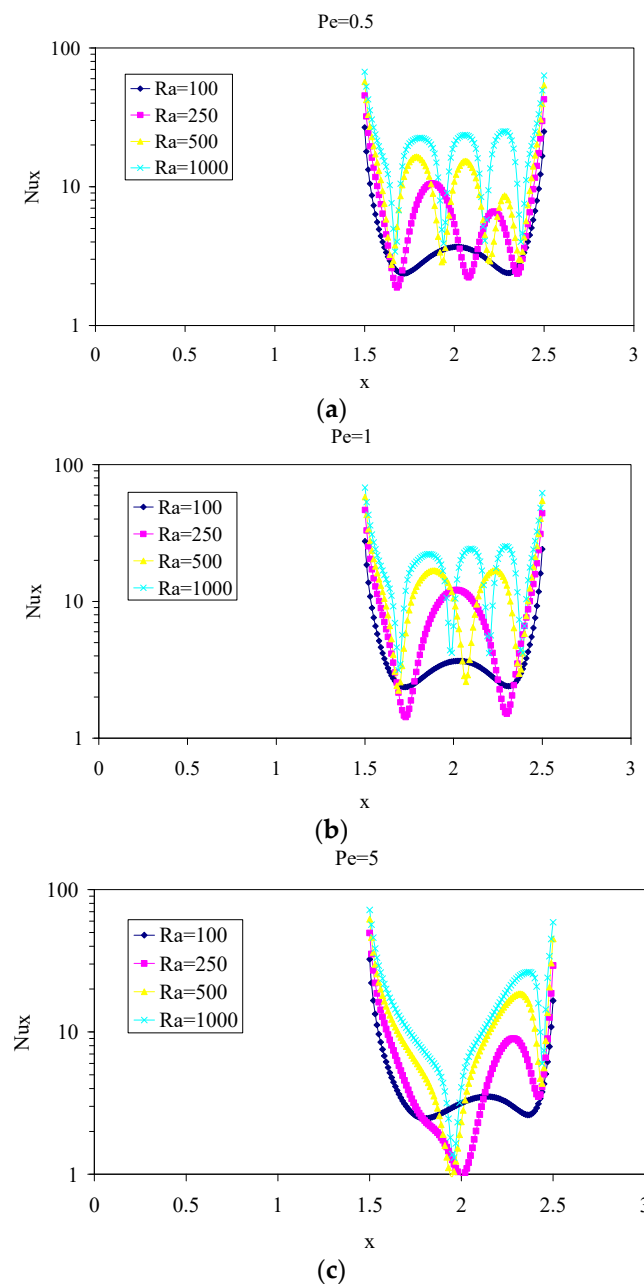


Figure 7. Variation of local Nusselt number along the channel ($c = 0.66$), (a) $Pe = 0.5$, (b) $Pe = 1$, (c) $Pe = 5$.

In Figure 8, it has been indicated that the average Nusselt number changes with the Rayleigh number for different Peclet numbers in the case that the heat source is close to down-stream, and that this change is linear. When the Peclet number is high, one sees that heat transfer decreases, and that forced convection becomes dominant. There is little in the way of change in the average Nusselt number due to the fact that conductive heat transfer is dominant when the Rayleigh number is low. The Nusselt numbers are very close to each other when the Rayleigh numbers are low, whereby the conductive heat transfer is dominant. The increase in the Rayleigh number leads to an increase in the maximum and minimum flow function values, especially by means of creating more centers of rotation around the heat source. This thus ensures the increase in the average Nusselt number by increasing the conductive heat transfer. Since the increase in Peclet number means an increase in the Reynolds number (i.e., the forced convection parameter ($Pe = Re Pr$)), the conductive heat transfer becomes dominant. Moreover, while the value of Nusselt number is high for $Pe = 5$, it is low for $Pe = 0.5$.

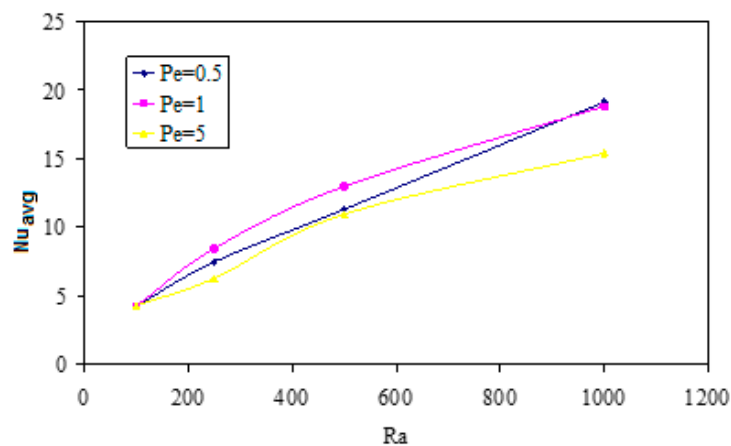


Figure 8. Variation of average Nusselt number with Rayleigh number ($c = 0.33$).

In Figure 9, it is indicated that the average number of Nu changes with the Ra number for different Pe numbers in the case that the heat source is close to the up-stream. The average Nusselt number increases almost linearly as the Rayleigh number increases. A nearly linear increase has been observed due to the conductive heat transfer being dominant in the low Ra numbers.

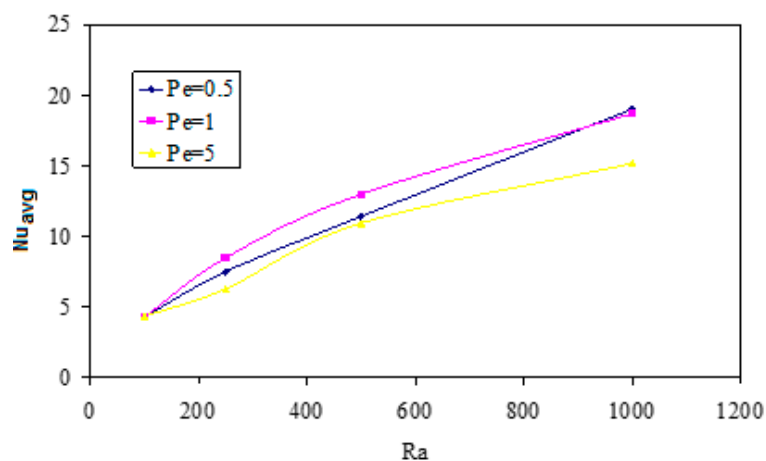


Figure 9. Variation of average Nusselt number with Rayleigh number ($c = 0.66$).

4. Conclusions

In this study, mixed convection heat transfer has been numerically studied in a channel filled with a porous medium with potentially negligible upper and bottom walls thickness. The numerical results are presented for the Rayleigh number range of $Ra = 100$ – 1000 for different Peclet numbers ($Pe = 0.5$ – 1 – 5). In view of the results presented, the main findings can be summarized as follows:

- For all Rayleigh numbers, a center of rotation forms around the heater within the volume.
- Heat transfer increases as the Rayleigh numbers increase.
- When the Peclet numbers are small, the free convection mode is dominant. When the Peclet numbers are large, the forced convection mode is dominant.
- The results from the governing equations show the oscillation of the average Nusselt number along the heated element.
- When the effects of Nusselt number for different heater positions among different Rayleigh numbers are examined, the local Nusselt number increases as the Rayleigh number increases for more energy inputs into the system. The Nusselt numbers are very close to each other when the Rayleigh numbers are low, and where conductive heat transfer is dominant.

- It is seen that heat transfer decreases when the Peclet number increases. However, when the Peclet number is low, heat transmission is more dominant than the heat convection in the flow medium.
- The results showed that increasing of the Rayleigh number enhanced the heat transfer for the same effective parameters.

Author Contributions: Conceptualization, F.O.; methodology, F.O.; investigation, F.O. and Y.V.; writing—original draft preparation, Y.V.; writing—review and editing, Y.V.

Funding: This research received no external funding.

Conflicts of Interest: The authors declare no conflict of interest and the funders had no role in the design of the study; in the collection, analyses, or interpretation of data; in the writing of the manuscript, or in the decision to publish the results.

Nomenclature

β	thermal expansion coefficient, $1/K$
g	gravitational acceleration, m/s^2
H^*	dimensionless height of the channel
K	ratio of thermal conductivity, ks/kf
L^*	dimensionless length of the channel
Nu_x	local Nusselt number
Nu	average Nusselt number
Pe	Peclet number
Ra	Rayleigh number
T	fluid temperature, K
T_h	bottom temperature of enclosure, K
T_c	upper temperature of enclosure, K
u, v	axial and radial velocities, m/s^2
U, V	dimensionless axial and radial velocities
x, y	Cartesian coordinates, m
X, Y	non-dimensional coordinates
W^*	dimensionless width of heat source
α	thermal diffusivity, m^2/s
ν	kinematic viscosity, m^2/s
θ	non-dimensional temperature
ψ	Stream function
Ψ	non-dimensional stream function

References

1. Jang, J.Y.; Chen, J.L. Variable porosity effect on vortex instability of a horizontal mixed convection flow in a saturated porous medium. *Int. J. Heat Mass Transf.* **1993**, *36*, 1573–1582. [\[CrossRef\]](#)
2. Aydın, O.; Kaya, A. Mixed convection of a viscous dissipating fluid about a vertical flat plate. *Appl. Math. Model.* **2007**, *31*, 843–853. [\[CrossRef\]](#)
3. Özgen, F.; Varol, Y.; Öztop, H.F. Numerical study of mixed convection in a horizontal channel filled with a fluid-saturated porous medium. *J. Therm. Sci. Technol.* **2013**, *33*, 155–163.
4. Sharma, A.K.; Bera, P. Linear stability of mixed convection in a differentially heated vertical channel filled with high permeable porous-medium. *Int. J. Therm. Sci.* **2018**, *134*, 622–638. [\[CrossRef\]](#)
5. Kumar, J.; Bera, P.; Khalili, A. Influence of inertia and drag terms on the stability of mixed convection in a vertical porous-medium channel. *Int. J. Heat Mass Transf.* **2010**, *53*, 5261–5273. [\[CrossRef\]](#)
6. Basak, T.; Krishna Pradeep, P.V.; Roy, S.; Pop, I. Finite element based heatline approach to study mixed convection in a porous square cavity with various wall thermal boundary conditions. *Int. J. Heat Mass Transf.* **2011**, *54*, 1706–1727. [\[CrossRef\]](#)
7. Xu, H.; Cui, J. Mixed convection flow in a channel with slip in a porous medium saturated with a nanofluid containing both nanoparticles and microorganisms. *Int. J. Heat Mass Transf.* **2018**, *125*, 1043–1053. [\[CrossRef\]](#)

8. Cimpean, D.S.; Pop, I. Fully developed mixed convection flow of a nanofluid through an inclined channel filled with a porous medium. *Int. J. Heat Mass Transf.* **2012**, *55*, 907–914. [[CrossRef](#)]
9. Moutsoglou, A.; Chen, T.S.; Cheng, K.C. Vortex instability of mixed convection flow over a horizontal flat plate. *J. Heat Transf.* **1981**, *103*, 257–261. [[CrossRef](#)]
10. Saeid, N.H.; Mohamad, A.A. Jet impingement cooling of a horizontal surface in a confined porous medium: Mixed convection regime. *Int. J. Heat Mass Transf.* **2006**, *49*, 3906–3913. [[CrossRef](#)]
11. Elbashbeshy, E.M.A. Laminar mixed convection over horizontal flat plate embedded in a non-Darcian porous medium with suction and injection. *Appl. Math. Comput.* **2001**, *121*, 123–128. [[CrossRef](#)]
12. Varol, Y.; Öztö, H.F.; Özgün, F.; Koca, A. Experimental and numerical study on laminar natural convection in a cavity heated from bottom due to an inclined fin. *Heat Mass Transf.* **2012**, *48*, 61–70. [[CrossRef](#)]
13. Kumari, M.; Nath, G. Radiation effect on mixed convection from a horizontal surface in a porous medium. *Mech. Res. Commun.* **2004**, *31*, 483–491.
14. Pop, I.; Rees, D.A.S.; Egbers, C. Mixed convection flow in a narrow vertical duct filled with a porous medium. *Int. J. Therm. Sci.* **2004**, *43*, 489–498. [[CrossRef](#)]
15. Guerroudj, N.; Kahalerras, H. Mixed convection in a channel provided with heated porous blocks of various shapes. *Energy Convers. Manag.* **2010**, *51*, 505–517. [[CrossRef](#)]
16. Khanafer, K.; Chamkha, A.J. Mixed convection within a porous heat generating horizontal annulus. *Int. J. Heat Mass Transf.* **2003**, *46*, 1725–1735. [[CrossRef](#)]
17. Muthuraj, R.; Srinivas, S. Mixed convective heat and mass transfer in a vertical wavy channel with traveling thermal waves and porous medium. *Comput. Math. Appl.* **2010**, *59*, 3516–3528. [[CrossRef](#)]
18. Kumari, M. Variable viscosity effects on free and mixed convection boundary-layer flow from a horizontal surface in a saturated porous medium variable heat flux. *Mech. Res. Commun.* **2001**, *28*, 339–348. [[CrossRef](#)]
19. Nosonov, I.I.; Sheremet, M.A. Conjugate mixed convection in a rectangular cavity with a local heater. *Int. J. Mech. Sci.* **2018**, *136*, 243–251. [[CrossRef](#)]
20. Saeid, N.H.; Pop, I. Transient mixed convection in a horizontal porous layer heated from below by isoflux heater. In Proceedings of the International Conference on Computational Heat and Mass Transfer, Cachan, France, 17–20 May 2005.
21. Saeid, N.H. Natural convection in porous cavity with sinusoidal bottom wall temperature variation. *Int. Commun. Heat Mass Transf.* **2005**, *32*, 454–463. [[CrossRef](#)]



© 2019 by the authors. Licensee MDPI, Basel, Switzerland. This article is an open access article distributed under the terms and conditions of the Creative Commons Attribution (CC BY) license (<http://creativecommons.org/licenses/by/4.0/>).